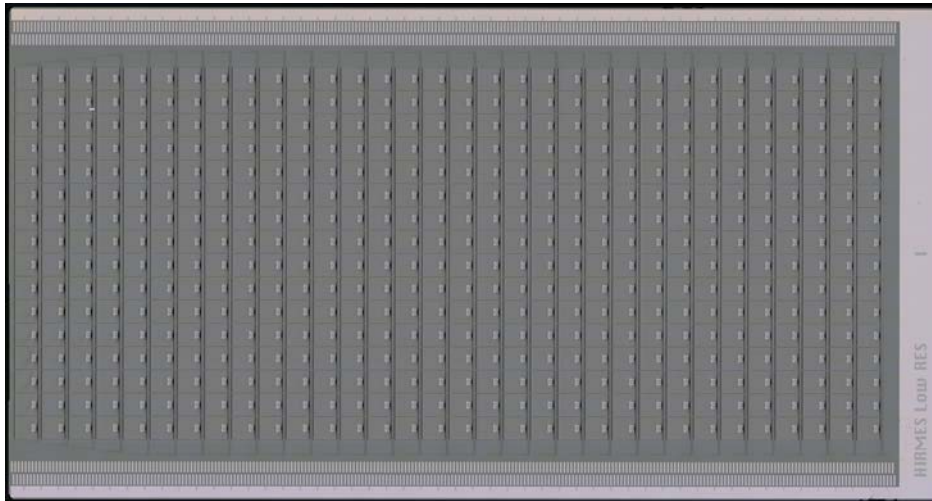


# Characterization of Si-membrane TES bolometer arrays for the HIRMES instrument



Please also  
see posters  
PC-18 & PC-19  
by Ari Brown

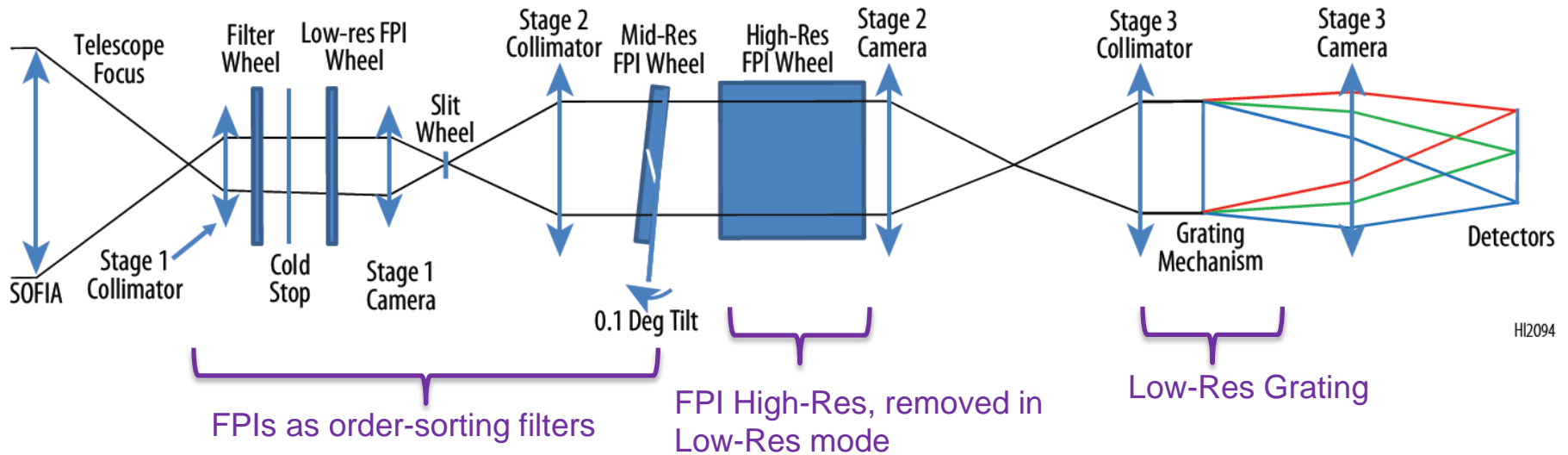
*Emily M. Barrentine, Karwan Rostem, Ari D. Brown, Regis P. Brekosky, Felipe A. Colazo, Nicholas P. Costen, Vorachai Kluengpho, Stephen F. Maher, Vilem Mikula, Timothy M. Miller, Joseph B. Oxborrow, Elmer H. Sharp, Tomomi Watanabe, James P. Hays-Wehle, Edward J. Wollack, Wen-Ting Hsieh, S. Harvey Moseley*

**NASA-Goddard Space Flight Center  
Greenbelt, MD, USA**

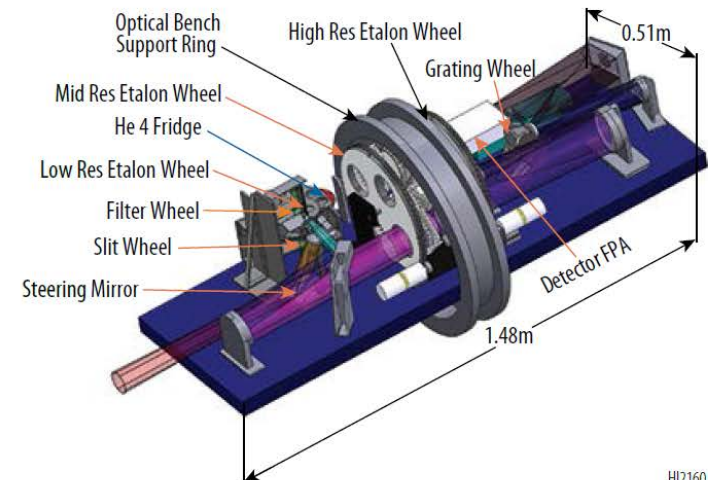
17<sup>th</sup> Annual Low-Temperature Detector Workshop, Kurume, Japan

July 18, 2017

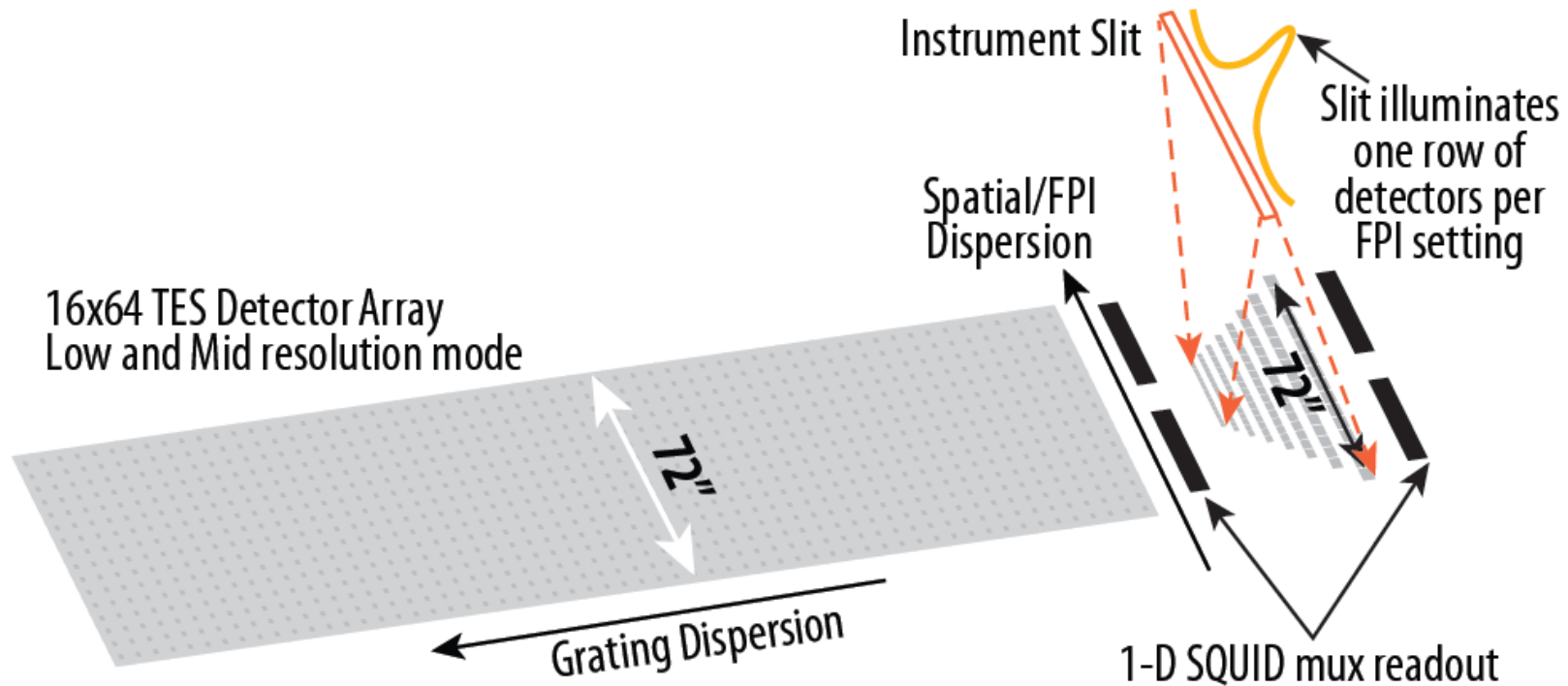
## The HIRMES Instrument & Science



- The High Resolution Mid-Infrared Spectrometer (HIRMES) instrument will fly onboard NASA's airborne Stratospheric Observatory for Infrared Astronomy (SOFIA) in 2019.
- HIRMES provides a unique observing window (25 – 122  $\mu\text{m}$ , H<sub>2</sub>O-vapor & ice, HD, OI) for exploring the composition and kinematics of protoplanetary disks and their evolution into young solar systems.
- Grating dispersive spectroscopy (for lower resolution operation mode) with addition of Fabry-Perot Interferometer (FPI) tunable narrow-band filters (for higher resolution operation mode).



## The HIRMES Focal Plane



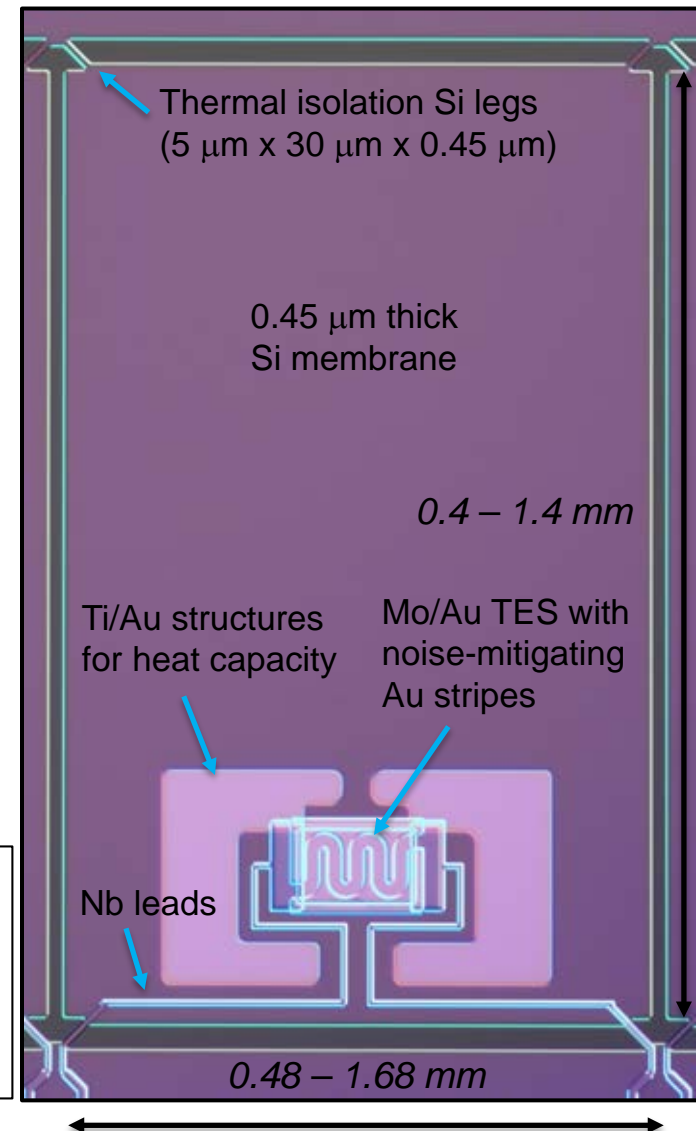
### Two focal plane detector arrays:

1. A high-resolution ( $\lambda/\Delta\lambda = 100,000$ )  $8 \times 16$  pixel array with pixel area optimized for each optical wavelength, with  $\text{NEP} \leq 3 \times 10^{-18} \text{ W}/\sqrt{\text{Hz}}$ .
2. A low-resolution ( $\lambda/\Delta\lambda = 2,000 - 19,000$ )  $16 \times 64$  pixel array with identical pixels optimized over a broadband, with  $\text{NEP} \leq 2 \times 10^{-17} \text{ W}/\sqrt{\text{Hz}}$ .

## Hi-Res Array Detector Design

- Mo/Au TES on a 0.45  $\mu\text{m}$  thick Si suspended membrane.
- Thermal conductance of Si isolation legs was designed following a diffusive-ballistic thermal transport model (K. Rostem et al. J. Appl. Phys. 2014):
  - ❖ Ballistic transport thermal conductance was calculated with COMSOL for single-crystal Si beams of fixed width and thickness.
  - ❖ A correction to account for a diffuse scattering fraction, dependent on the beam length and top and sidewall beam roughness was then applied.
- The Debye heat capacity of the Si membrane is very small, thus metallic Ti/Au structures are added to define the detector heat capacity and to ensure stability.
- NbTiN absorber coating with a quarter-wave reflective backshort.

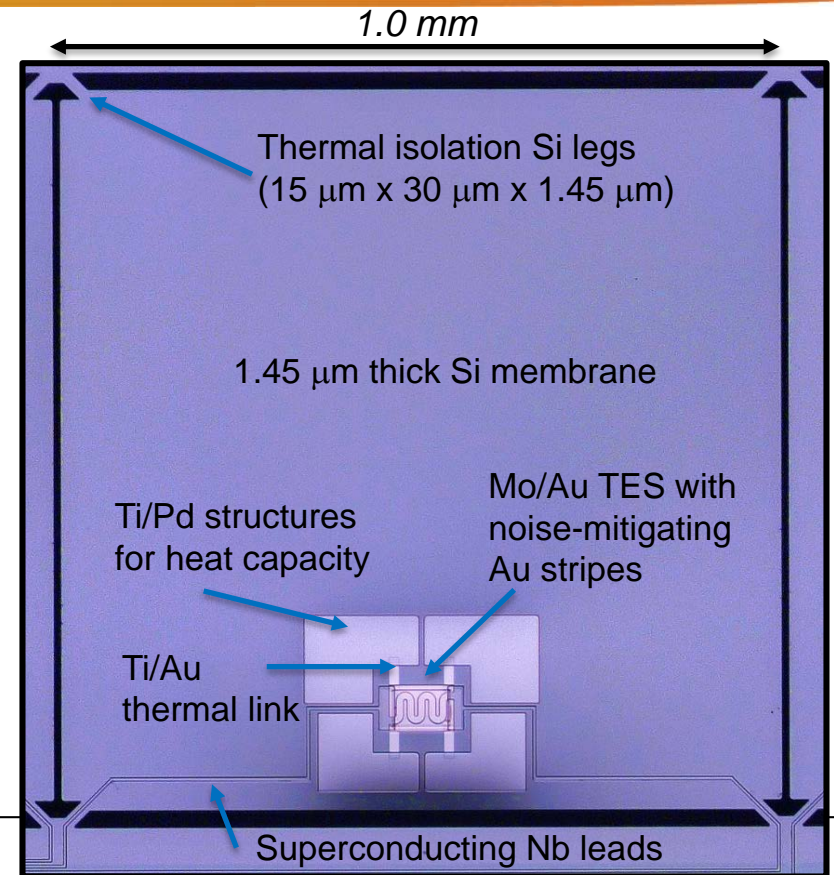
Design Targets:  $T_c = 110 \text{ mK} \pm 10 \text{ mK}$   
 $G(T_c) = 6 \text{ pW/K}$   
 $\text{NEP} < 3 \times 10^{-18} \text{ W/Hz}^{1/2}$  (photon background  $\sim 8 \times 10^{-18} \text{ W/Hz}^{1/2}$ )  
 Saturation power =  $0.2 \text{ pW} \pm 0.05 \text{ pW}$  @ 70 mK base temp  
 Time constant  $\sim 5 \text{ ms}$   
 Optical efficiency  $> 90\%$





## Low-Res Array & Detector Design

- A 64x16 detector array consisting of two 32x16 arrays of identical pixels.
- Mo/Au TES on a 1.45  $\mu\text{m}$  thick Si suspended membranes.
- Like the Hi-Res arrays, the thermal conductance of Si isolation legs was designed following a diffusive-ballistic thermal transport model (K. Rostem et al. J. Appl. Phys. 2014).
- The Debye heat capacity of the Si membrane is very small, thus metallic Ti/Pd structures are added to define the detector heat capacity and ensure stability.
- A  $\text{Mo}_2\text{N}$  absorber-coating, with no reflective backshort for broadband optical efficiency.



Design Targets:  $T_c = 165 \text{ mK} \pm 10 \text{ mK}$

$G(T_c) \sim 200 \text{ pW/K}$

$\text{NEP} < 2 \times 10^{-17} \text{ W/Hz}^{1/2}$  (photon background  $\sim 3 \times 10^{-17} \text{ W/Hz}^{1/2}$ )

Saturation power: Original design  $\sim 12 \text{ pW}$  @ 70 mK base temp

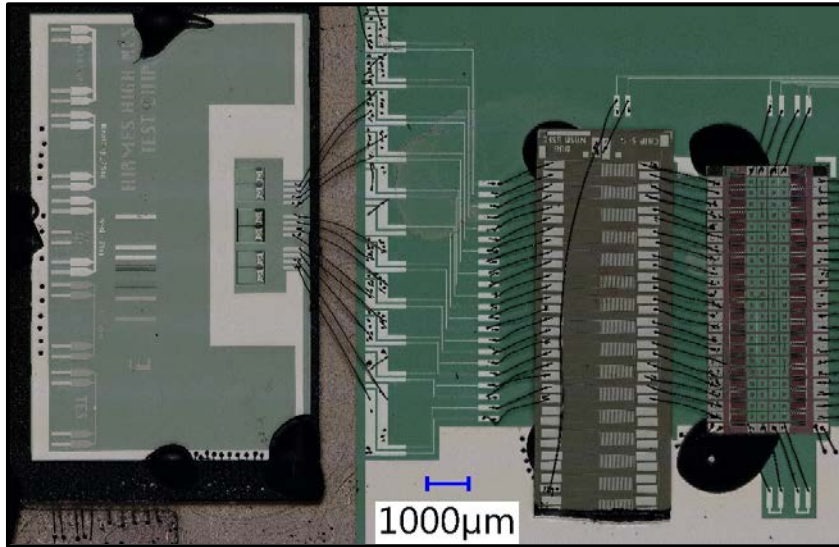
Updated design = 18 pW @ 70 mK base temp due to change in optical design (due to this &

missing  $T_c$  target we are exploring leg metallization – see later slides)

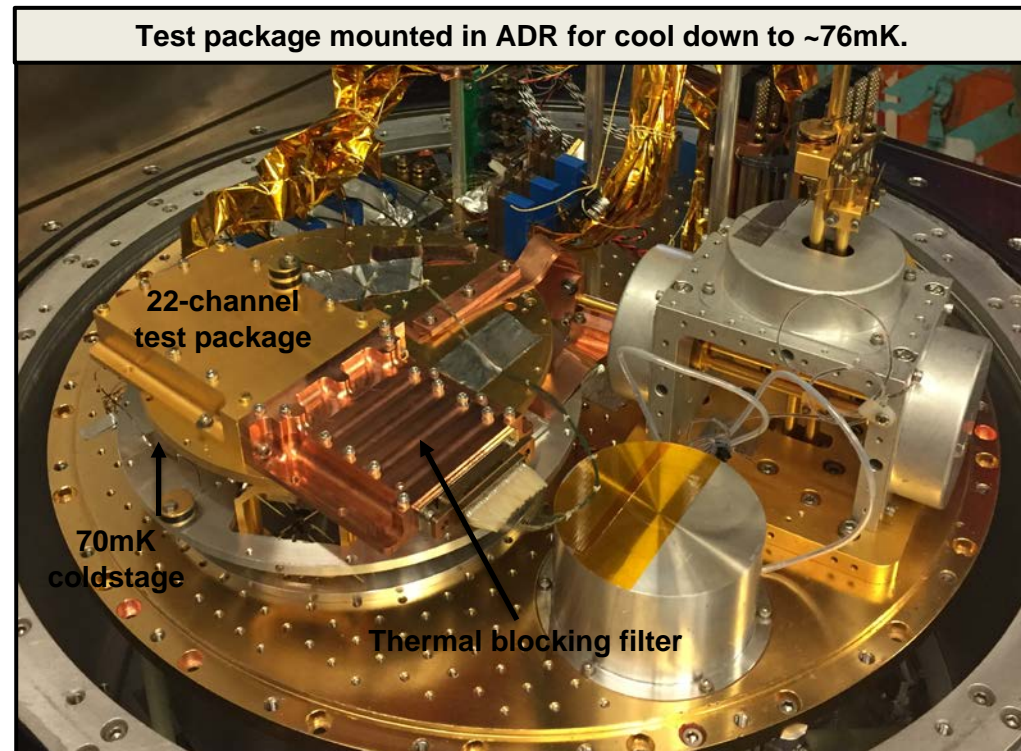
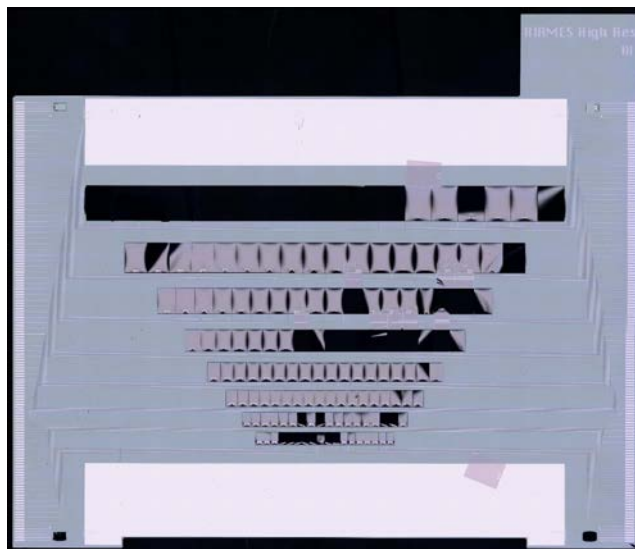
Time constant:  $\sim 5 \text{ ms}$

Optical efficiency  $> 45\%$  (50% by design)

## Hi-Res Detector Characterization



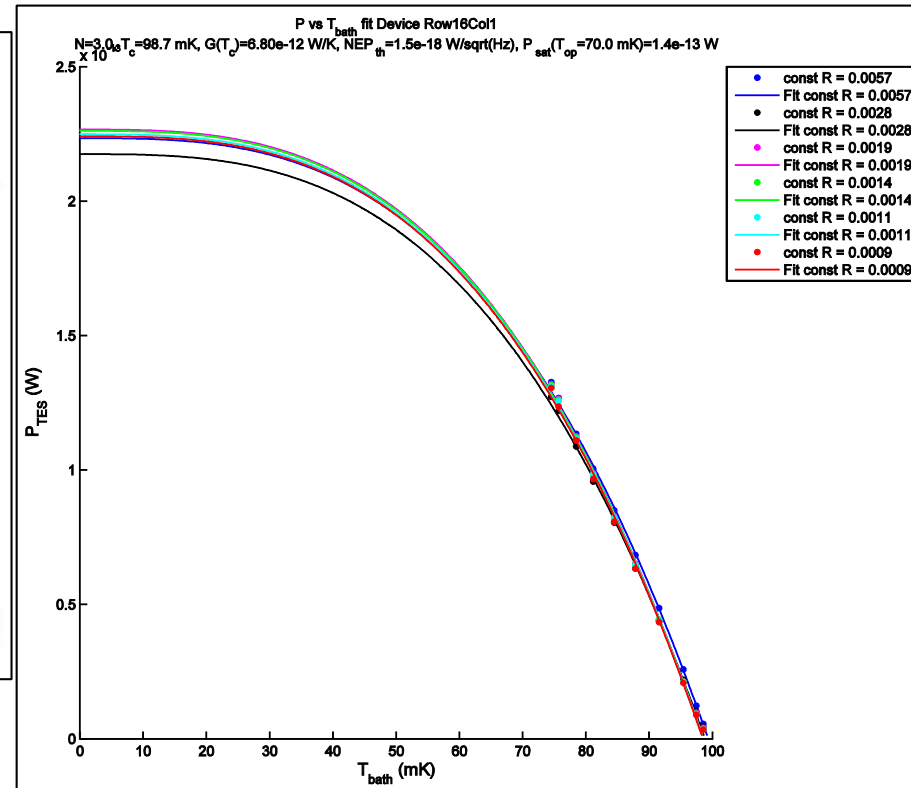
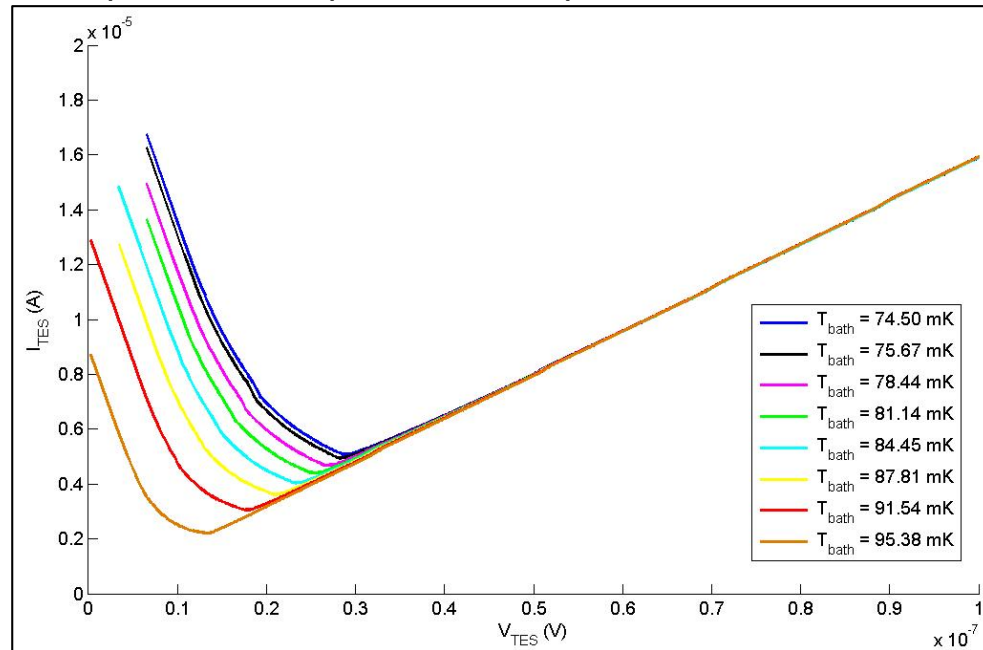
- We have completed dark tests of two test chips without absorber coating (including 3 variations of leg designs) as well as testing one of the first realized (low-yield) full arrays with absorber coating.
- With absorber coating we found that, in addition to thermal blocking filters, we had to add blackening to the package lid and sealing to avoid saturation.





## Hi-Res Array Detector Performance

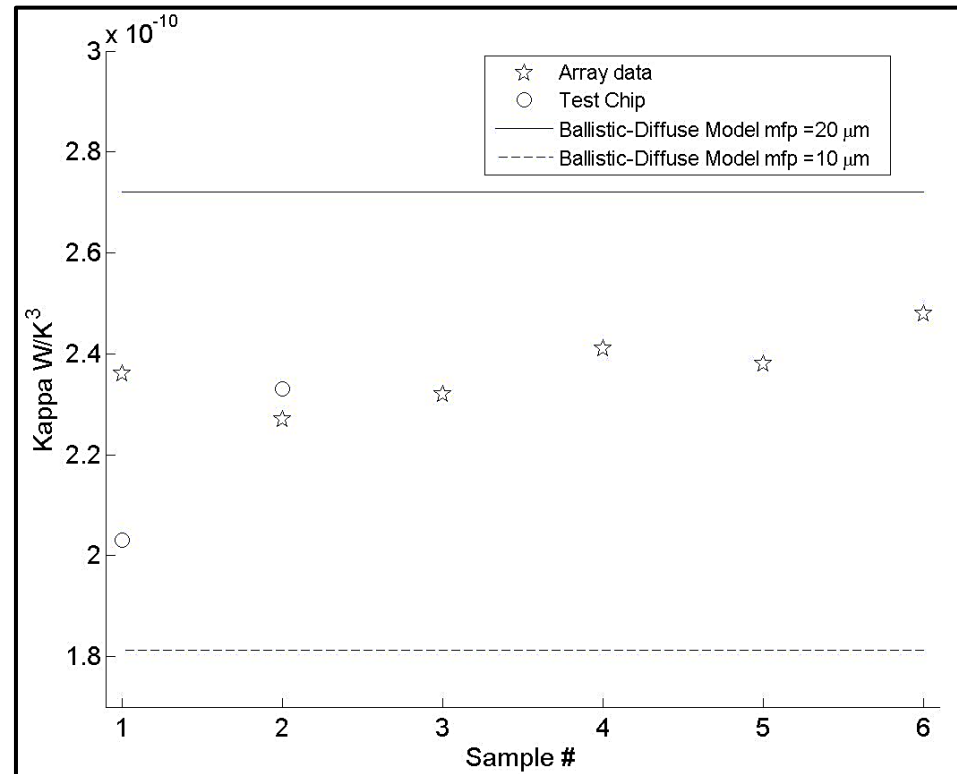
Example of I-V temperature sweep for one TES device:



- $T_c \sim 99 \text{ mK}$ , at low end, but within design tolerance.
- Fitting to  $P = \text{Kappa} \cdot (T_c^n - T_{\text{bath}}^n)$  found consistent fits with  $n \sim 3$  or  $G \sim T^2$  (expected from diffusive-ballistic model).
- Saturation power at 70 mK base temperature is  $\sim 0.14 \text{ pW}$  about  $\sim 70\%$  of the design target value, but will meet requirements. Note (see next slide) the discrepancy from design target is due to  $T_c$  and not Kappa.
- Expected thermal fluctuation noise at 70 mK is  $\sim 1.5 \times 10^{-18} \text{ W/sqrt(Hz)}$ , below the required upper limit of  $3 \times 10^{-18} \text{ W/sqrt(Hz)}$ . This noise level is also consistent with our preliminary analysis of dark NEP measurements of these devices.

## Hi-Res Array Thermal Conductance

Comparison of thermal conductance measurements for nominal leg design length of 20 microns (from a single wafer), shows agreement to our diffusive-ballistic model:

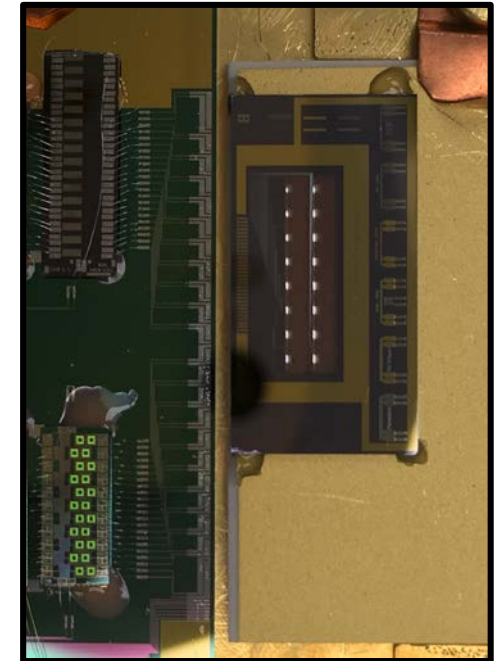
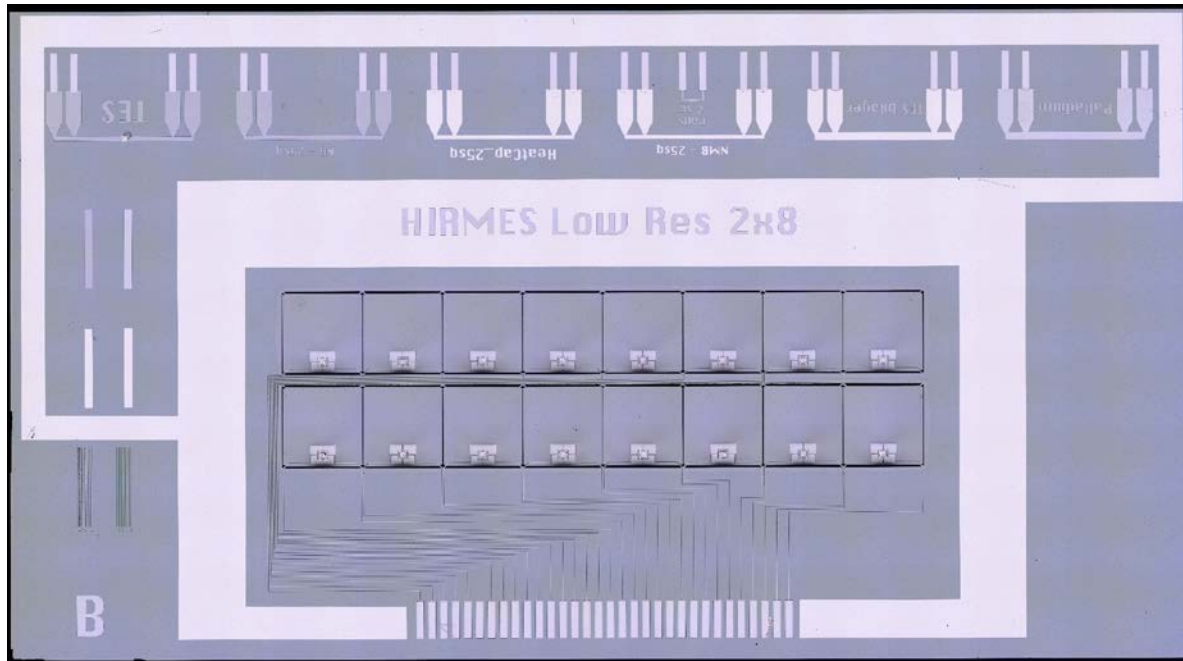


No. of Silicon Beams per Mem. G @ target Tc x4 Beams		4		15.04 [pW/K]		Target L		
m.f.p [um]		L [um]	10	15	20	25	30	35
5		5.01	3.76	3.01	2.51	2.15	1.88	
10		7.52	6.02	5.01	4.30	3.76	3.34	
15		9.02	7.52	6.45	5.64	5.01	4.51	
20		10.03	8.59	7.52	6.68	6.02	5.47	
25		10.74	9.40	8.36	7.52	6.84	6.27	
30		11.28	10.03	9.02	8.20	7.52	6.94	
35		11.70	10.53	9.57	8.77	8.10	7.52	

$$P = \text{Kappa} * (T_c^n - T_{\text{bath}}^n)$$



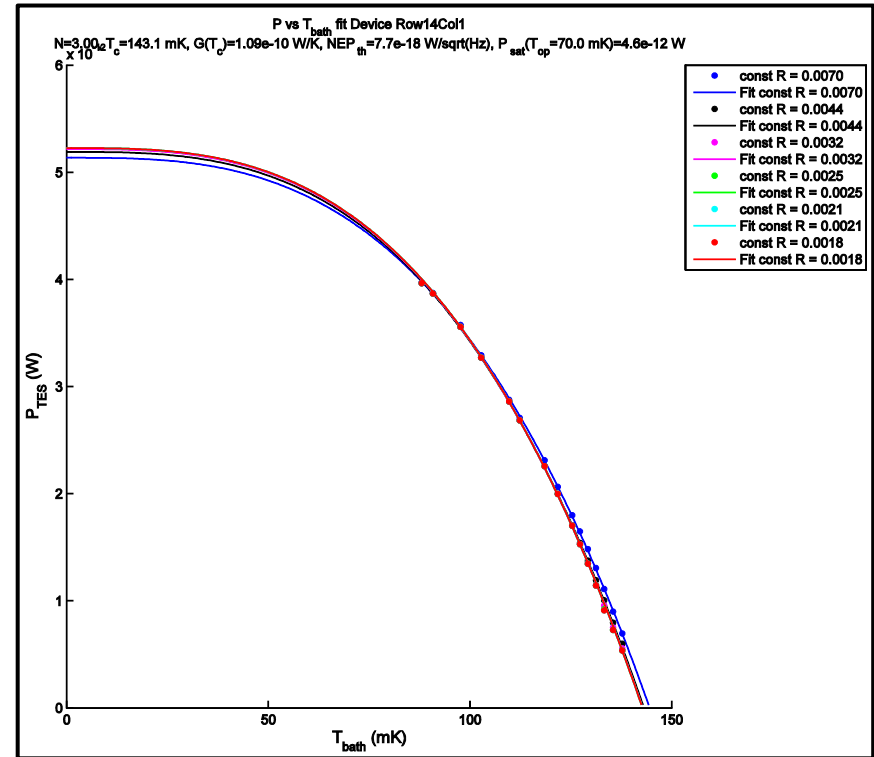
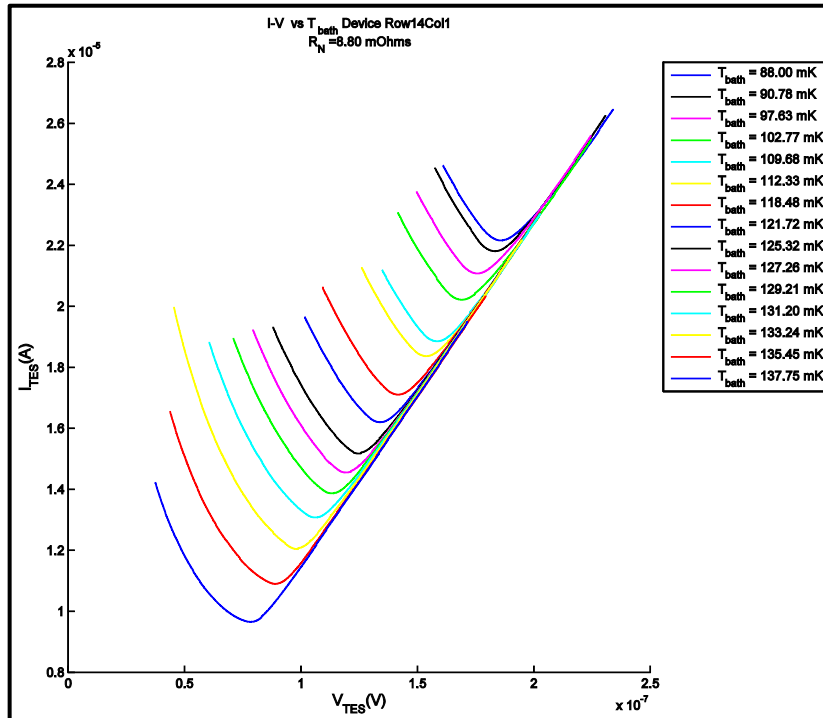
## Low-Res Detector Characterization



- We have characterized two 2x8 Low-Res test chip arrays without absorber coatings from two wafers.
- These devices were characterized in a dark environment identical to environment for testing the Hi-Res test devices.

## Low-Res Array Detector Performance

Example of I-V temperature sweep for one TES device:



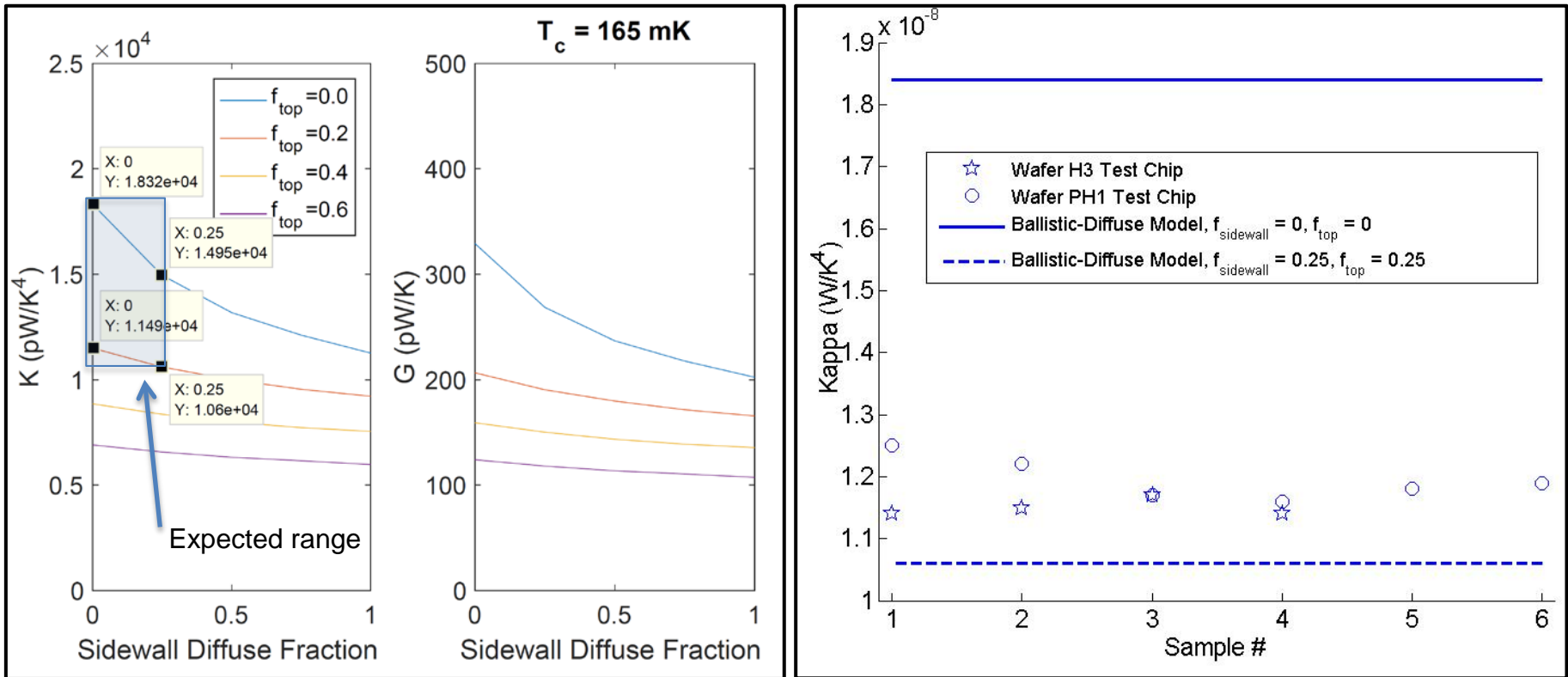
- $T_c = 145\text{--}150$  mK which is 5 mK below design tolerance.
- Fitting to  $P = \text{Kappa} \cdot (T_c^n - T_{\text{bath}}^n)$  is consistent with  $n \sim 4$  or  $G \sim T^3$  (expected from our diffusive-ballistic model) but obtain slightly better fits at the lowest temperature data points for  $n \sim 3$  or  $G \sim T^2$ .
- Saturation power at 70 mK operation temperature is  $\sim 4\text{--}7$  pW about  $\sim 50\%$  of design target of 12 pW, and will not meet new requirement of 18 pW – we are currently exploring PdAu metallization of legs to increase G.
- Expected thermal fluctuation noise is  $\sim 8 \times 10^{-18}$  to  $1 \times 10^{-17}$  W/sqrt(Hz), below required upper limit of  $3 \times 10^{-18}$  W/sqrt(Hz).

## Low-Res Detector Thermal Conductance

Model:

$$P = \text{Kappa} * (T_c^n - T_{\text{bath}}^n)$$

Test Device Measurements  
( $T_c = 141\text{--}150\text{ mK}$ ):

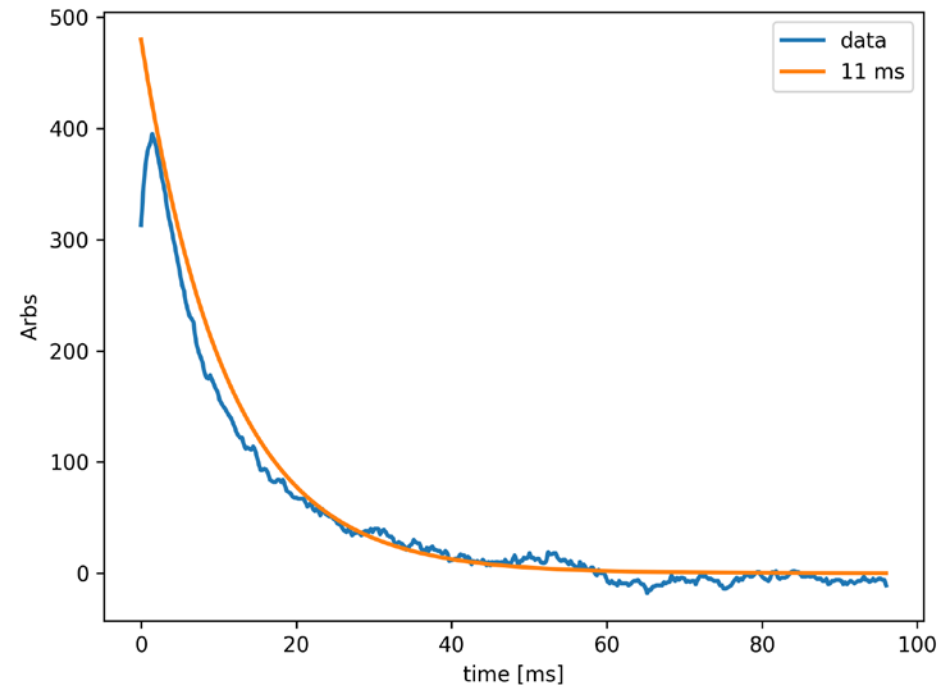
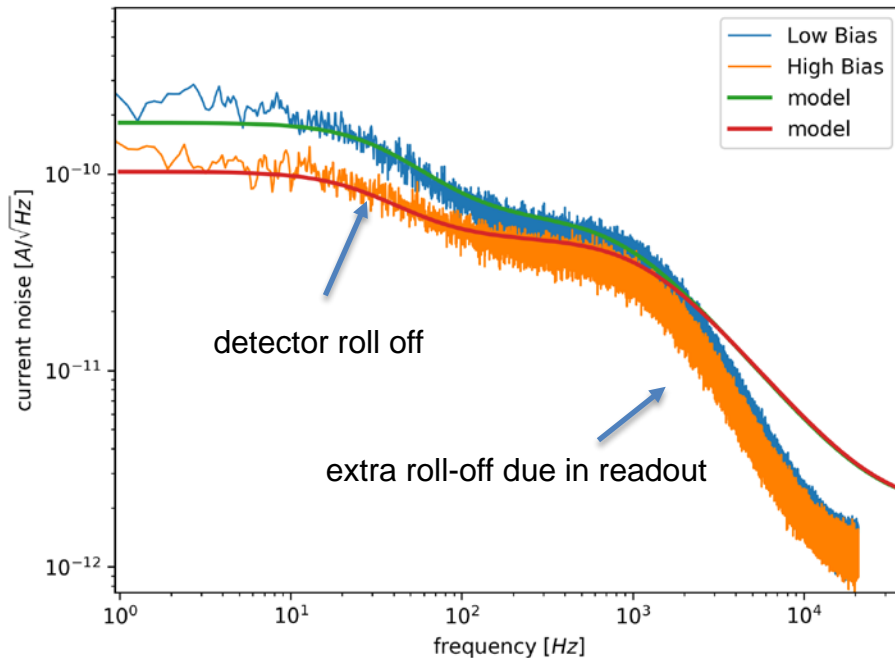


Comparison of thermal conductance measurements from two wafers shows agreement to our diffusive-ballistic model, but towards the low end of the expected range.



## Low-Res Array Performance

Example of dark noise and time constant measurements from a single pixel:



- From our preliminary analysis this current noise level is consistent with our design parameters, and a dark NEP at phonon noise levels.
- Detector time constant  $\sim 10$  ms

## ***HIRMES Detector Validation Status***

- The Hi-Res thermal detector design has been validated (thermal conductance,  $T_c$  and saturation power, NEP) on test chips.
- The Low-Res detector design G and NEP have been validated, however, modification of the thermal design is required to meet new saturation power requirements.
- Future test device validation:
  1. Hi-Res devices with improved optical coupling strategy (see poster PC-19)
  2. Low-Res devices with metallization of the thermal isolation legs (in progress)
  3. Low-Res devices with absorber
- Once test devices from an array wafer meet requirements, we will begin integration of the detector arrays from these wafers into the flight package, for dark and optical testing.

Thank you!

ありがとうございます



backup

# HIRMES Science Goals

The High-Resolution Mid-Infrared Spectrometer (HIRMES) addresses fundamental questions about the evolution of planetary systems, answering questions such as:

- **How does the disk mass evolve during planetary formation?**
- **What is the distribution of oxygen, water ice, and water vapor in different phases of planet formation?**
- **What are the kinematics of water vapor and oxygen in protoplanetary disks?**

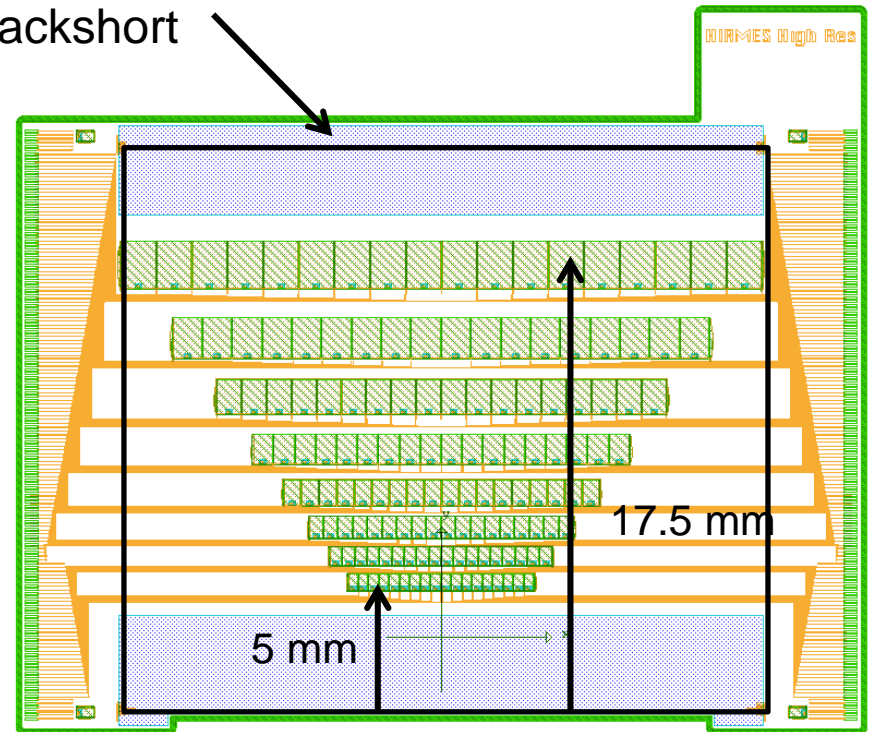
Driving Science Goal	Science Requirements	Required Measurement	Required Observations	Instrument Requirement
<b>Study of Protoplanetary Disks</b> <ul style="list-style-type: none"> <li>• What are the processes through which protoplanetary disks evolve into nascent planetary systems?</li> <li>• What is the origin and ultimate fate of water in the planet forming regions of protoplanetary disks?</li> <li>• What is the spatial structure of protoplanetary disks in the region of planet formation?</li> </ul>	<b>Measure the mass, composition, and kinematics of protoplanetary disks</b>	Determine the disk gas mass & kinematics	HD 1-0 R(0) line 112.0725 $\mu\text{m}$	R ~ 100,000 (3 km s <sup>-1</sup> ) Scan range: 15 km s <sup>-1</sup> Sensitivity: $\leq 10^{-17}$ W m <sup>-2</sup> 5 $\sigma$ in 1 hour Absolute $\lambda$ accuracy: 0.1 $\Delta\lambda$
		Determine the amount of O and H <sub>2</sub> O inside snowline	[OI] line 63.1837 $\mu\text{m}$ Warm H <sub>2</sub> O 28-38 $\mu\text{m}$	R ~ 50,000 (6 km s <sup>-1</sup> ) Scan range: 30 km s <sup>-1</sup> Sensitivity: $\sim 10^{-17}$ W m <sup>-2</sup> 5 $\sigma$ in 1 hour Absolute $\lambda$ accuracy: 0.1 $\Delta\lambda$
		Determine the amount of H <sub>2</sub> O-ice beyond snowline	Measure the solid-state H <sub>2</sub> O-ice features at $\sim 43$ $\mu\text{m}$ and $\sim 63$ $\mu\text{m}$	Acquire complete spectrum from 35-70 $\mu\text{m}$ at R = 100, with 0.04 Jy 1 $\sigma$ noise over full range Absolute $\lambda$ accuracy: 0.2 $\Delta\lambda$
<b>H and D in the Solar System</b> <ul style="list-style-type: none"> <li>• What is the origin of the constituent materials of the Solar System? Does all of the material have common origin, or were there variations in characteristics across the Solar nebula?</li> </ul>	<b>Determine the isotopic composition of the constituents giant planets</b>	Determine the H/D ratio	Measure: H <sub>2</sub> S(0) at 28.221 $\mu\text{m}$ HD R(0) at 112.0725 $\mu\text{m}$ HD R(1) at 56.2298 $\mu\text{m}$ HD R(2) at 37.7015 $\mu\text{m}$ HD R(3) at 28.5020 $\mu\text{m}$	R ~ 10,000 Sensitivity: $< 5 \times 10^{-16}$ W m <sup>-2</sup> (Set by Neptune, the giant planet with the lowest flux density) Absolute $\lambda$ accuracy: 0.1 $\Delta\lambda$

## Hi-Res Array Design

An 8x16 array consisting of rows of pixels of sizes from ~0.4-1.5 mm:

Row	Waveband [ $\mu\text{m}$ ]	Back short spacing [ $\mu\text{m}$ ]	Distance between edge of backshort and pixels [mm]
1	30.0	7.5	5
2	35.9	9.0	6
3	42.9	10.7	7.13
4	51.3	12.8	8.53
5	61.4	15.3	10.2
6	73.4	18.4	12.3
7	87.8	21.9	14.6
8	105	26.3	17.5

Wedged  $\lambda_0/4$   
Backshort



Please see Ari Brown's poster PC-19 for more on the absorber design



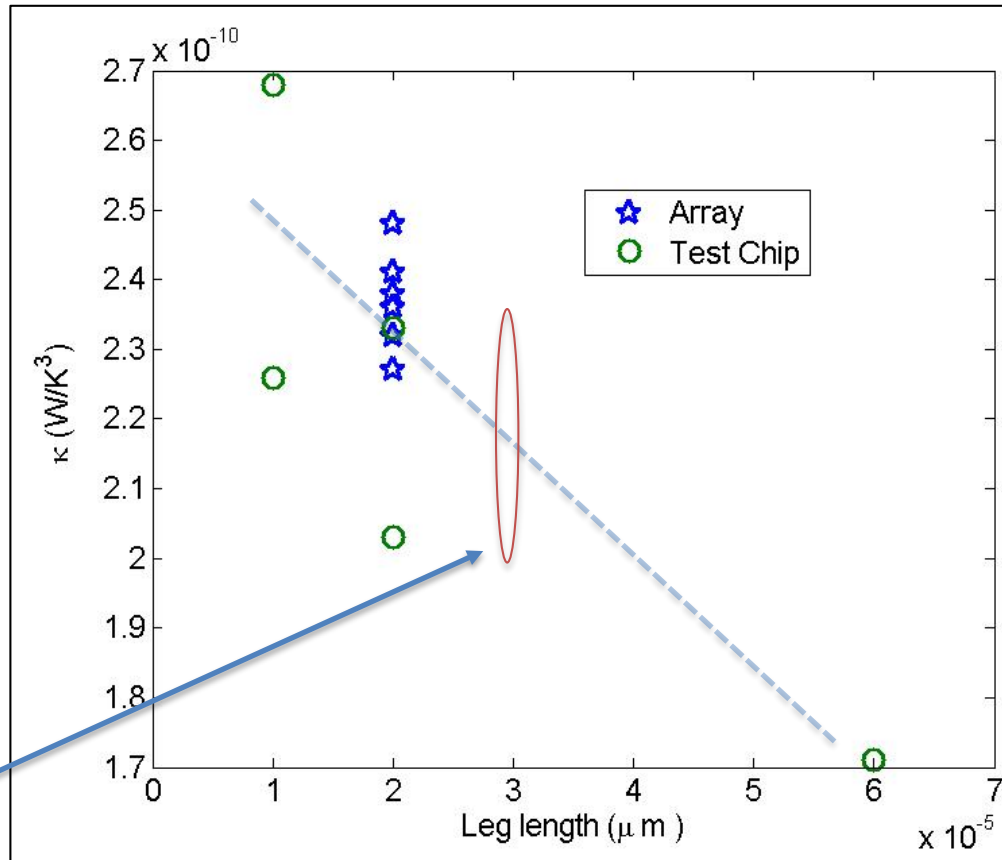
# Hi-Res Array Detector Performance cont.

Table comparison of all pixels tested from lead Hi-Res Wafer R08:

Chip Label	Leg Design	MCE R,C	$R_{shunt}$ (m $\Omega$ )	$R_N$ (m $\Omega$ )	$T_c$ (mK) n=3	Kappa (W/K <sup>N</sup> ) n=3	G (Tc) (pW/K) n=3 fit	$P_{sat}$ (pW) @ 70mK n=3 fit	NEP <sub>thermal</sub> (W/sqrt(Hz)) @ 70mK Predicted by Kappa, n=3
G	5x20um	9,0	0.73	6.3	98.3	2.03e-10	5.89	0.123	1.38e-18
G	5x20um	16,1	1.04	6.3	98.7	2.33e-10	6.80	0.144	1.49e-18
G	5x60um	17,1	1.04	6.3	98.7	1.71e-10	4.99	0.106	1.28e-18
G	5x10um	19,1	1.04	6.3	99.2	2.68e-10	7.91	0.170	1.61e-18
G	5x10um	20,1	1.04	6.3	98.6	2.26e-10	6.59	0.139	1.46e-18
Array	5x20um	10,1	0.98	6.6	102	2.36e-10	7.31	0.167	1.57e-18
Array	5x20um	14,1	0.98	7.2	101	2.27e-10	6.90	0.154	1.52e-18
Array	5x20um	15,1	0.98	6.4	98.7	2.32e-10	6.64	0.137	1.46e-18
Array	5x20um	16,1	0.98	6.3	97.9	2.41e-10	6.94	0.143	1.50e-18
Array	5x20um	17,1	0.98	6.4	98.4	2.38e-10	6.90	0.145	1.50e-18
Array	5x20um	18,1	0.98	6.4	98.5	2.48e-10	7.22	0.152	1.53e-18

## Hi-Res Array Thermal Conductance

Kappa vs. leg length:



$$P = \text{Kappa} * (T_c^n - T_{\text{bath}}^n)$$

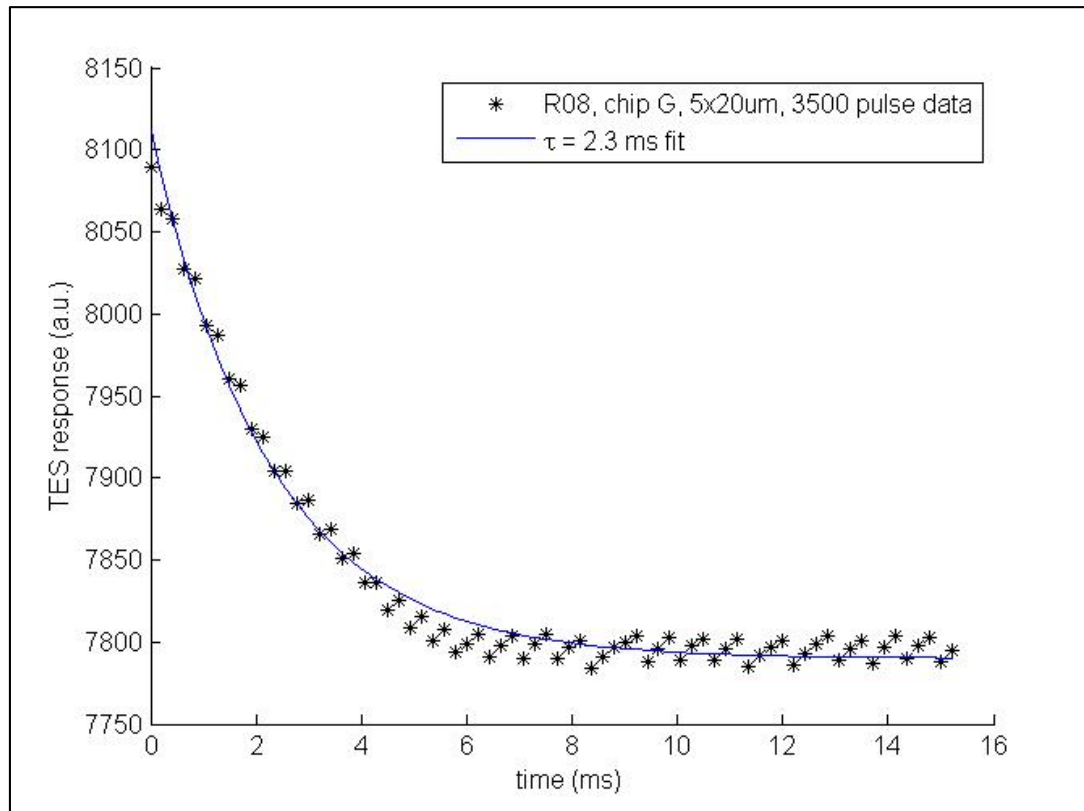
Leg width = 5  $\mu\text{m}$

Leg thickness = 0.45  $\mu\text{m}$

Based on these results, we decided to target a 30  $\mu\text{m}$  leg length for flight array wafers, for improved mechanical yield. Note, however, we expect a similar  $G(T_c=99\text{mK}) \sim 5\text{-}7 \text{ pW/K}$  & saturation power.

## Hi-Res Array Detector Performance cont.

Sending in small-square wave bias signal at bias in the transition region to measure electrothermal detector time constant with feedback directly for a test device without absorber coating:



Preliminary data show an increase in time constant likely due to added heat capacity with NbTiN film coating. This increase scaled with detector area – we believe this likely due to Two-Level systems in the NbTiN film. Current trials underway to deposit a more metallic-NbTiN coating.

# Low-Res Array Detector Performance

n = 3 values

Chip Label	Device #	MCE R,C	R <sub>shunt</sub> (mΩ)	R <sub>N</sub> (mΩ)	T <sub>c</sub> (mK) N=3	Kappa (W/K <sup>N</sup> ) N=3	G (Tc) (pW/K) N=3 fit	P <sub>sat</sub> (pW) @ 70mK N=3 fit	NEP <sub>thermal</sub> (W/sqrt(Hz)) @ 70mK Predicted by Kappa, N=3
PH1 Chip A	1	3,0	0.74	8.84	152	2.07e-09	143	6.6	9.3e-18
PH1 Chip A	3	5,0	0.74	8.74	152	2.00e-09	138	6.3	9.1e-18
PH1 Chip A	4	6,0	0.74	8.77	152	1.91e-09	132	6.0	8.9e-18
PH1 Chip A	5	7,0	0.74	8.81	150	1.89e-09	128	5.8	8.7e-18
PH1 Chip A	6	8,0	0.74	8.75	151	1.94e-09	133	6.0	8.9e-18
PH1 Chip A	7	9,0	0.74	8.86	151	1.96e-09	134	6.1	9.0e-18
H3 Chip B	9	11,1	1.04	8.8	144	1.79e-09	110	4.7	7.8e-18
H3 Chip B	10	12,1	1.04	8.8	143	1.79e-09	109	4.6	7.7e-18
H3 Chip B	12	13,1	1.04	8.8	143	1.83e-09	111	4.7	7.8e-18
H3 Chip B	14	14,1	1.04	8.8	143	1.77e-09	109	4.6	7.7e-18



# Low-Res Array Detector Performance

n = 4 values

Chip Label	Device #	MCE R,C	R <sub>shunt</sub> (mΩ)	R <sub>N</sub> (mΩ)	T <sub>c</sub> (mK) N=4	Kappa (W/K <sup>N</sup> ) N=4	G (Tc) (pW/K) N=4 fit	P <sub>sat</sub> (pW) @ 70mK N=4 fit	NEP <sub>thermal</sub> (W/sqrt(Hz)) @ 70mK Predicted by Kappa, N=4
PH1 Chip A	1	3,0	0.74	8.84	151	1.25e-08	171	6.2	1.0e-17
PH1 Chip A	3	5,0	0.74	8.74	150	1.22e-09	165	5.9	9.8e-18
PH1 Chip A	4	6,0	0.74	8.77	150	1.17e-08	159	5.7	8.9e-18
PH1 Chip A	5	7,0	0.74	8.81	149	1.16e-08	153	5.4	9.4e-18
PH1 Chip A	6	8,0	0.74	8.75	150	1.18e-08	158	5.6	9.6e-18
PH1 Chip A	7	9,0	0.74	8.86	150	1.19e-08	160	5.7	9.6e-18
H3 Chip B	9	11,1	1.04	8.8	142	1.14e-08	131	4.4	8.3e-18
H3 Chip B	10	12,1	1.04	8.8	141	1.15e-08	129	4.3	8.2e-18
H3 Chip B	12	13,1	1.04	8.8	141	1.17e-08	131	4.4	8.3e-18
H3 Chip B	14	14,1	1.04	8.8	141	1.14e-08	128	4.3	8.2e-18